Energetic and Exergetic Analyses of Biomass Derived Syngas for Triple Cycle Power Generation

Faizan Ahmad, Abdul Khaliq, Mohammad Idrees

ABSTRACT

To rise the thermal efficiency of power generation systems and to meet stricter environmental regulations, improved system integration based on renewable energy is a viable option. In this context, a syngas fuelled Brayton/Rankine combined power cycle integrated with the Organic Rankine Cycle (ORC) is proposed and analysed from both energetic and exergetic point of views. A thermo-chemical model was developed to predict the composition of syngas produced after biomass gasification, and also, a thermodynamic model was developed, to determine the energetic and exergetic performance of the proposed triple cycle power generation system. We show that both first-law and second-law efficiencies of triple power cycle decreases with the increase in pressure ratio and increases with higher gas turbine inlet temperature. It is further shown that first-law and second-law efficiencies of solid-waste-derived syngas fuelled triple power cycle are considerably higher than the rice husk derived syngas fuelled cycle. The worst performing components from irreversibility point of view in the proposed triple cycle are the combustor, Heat Recovery Steam Generator (HRSG), and gasifier, respectively. Our results show that integration of ORC with the Biomass-Fuelled Integrated Gasification Combined Cycle (BIGCC) is very effective in improving the thermal performance of the power plant and in reducing external waste emissions.

Keywords: gasification, synthetic gas, combined cycle, ORC, triple power cycle, energetic, exergetic

INTRODUCTION

Energy plays a vital role in the development and economic growth of every nation. Due to sheer increase in world population and living standards, world energy demand is increasing steadily which is majorly meeting out by the combustion of fossil fuels that result in their fast depletion and environmental degradation. This hastened the search for alternative energy sources like; solar, biomass, hydro, wind, tidal, geothermal etc. Among all these alternative sources of energy, biomass is the second largest source of renewable energy and is a biological material that comprises all the living matter present on earth and, as an energy source, biomass can either be used directly, or converted into other energy products like biofuels. Direct combustion of biomass is the most conventional method of energy conversion as it results in higher emissions of oxides of carbon and unburned hydrocarbons and provides a lower thermal efficiency. Another thermo-chemical conversion technology is the biomass gasification which is technically feasible, sustainable, and potentially efficient for power generation [1, 2].

Integrated gasification combined cycle (IGCC) is considered as one of the most important power generation system for future coal/biomass utilizations and is being promoted throughout the world as it provides higher efficiencies at reduced emissions. The superimposition of Brayton cycle over the Rankine cycle can result in overall thermal efficiencies of integrated gasification combined cycle (IGCC) power plants in excess of 45%. The gasification of biomass materials requires minimal fuel processing and its application in combined cycle plants provides a sustainable power generation [3, 4].

A method of exergy analysis, which has been found as a useful method in the design, evaluation, optimization and improvement of thermal power plants and is widely gaining acceptance over traditional energy methods in both industry and academia has been applied to BIGCC power plants by many investigators and there is literature based on exergy analysis of biomass fuelled combined gas-steam power cycles for various operating conditions. Mark and Mike [5] discussed the use of biomass gasification process as the key element in an advanced gas turbine system. Based on exergy analysis, Prins et al. [6] found that main exergy losses occur during biomass gasification, which accounted over 50% of the total losses. They reported that these exergy losses can be reduced if oxygen or enriched air is considered

for the gasification process. Ptasinski et al. [7] compared different types of bio fuels for their gasification efficiency and evaluated for exergy efficiency. Rutherford [8] modeled a biomass gasifier and investigated the effects of steam-fuel ratio and moisture content in biomass without taking solmodeledn content in the synthetic gas. Bhattacharya et al. [9] conducted a thermodynamic analysis of biomass integrated gasification combined cycle considering the combustion of supplementary biomass fuel using the oxygen available in gas turbine exhaust. Their results show the plant efficiencies increase with higher pressure and temperature ratios. They also evaluated the exergetic efficiency of plant's various equipment to localize the major thermodynamic irreversibilities in the plant. Fagbenle et al. [10] presented an analysis based on first and second laws of thermodynamics for a 53 MW biomass fuelled integrated gasification combined power cycle. Their analysis indicates that the exergy loss in the combustion chamber is the largest at about 79% of the total system exergy loss. Most of the BIGCC power plants investigated by the above authors achieved around 40% efficiency which is significantly lower than the thermodynamic efficiency of natural gas fuelled combined power cycles (50% to 57%). This lower range of efficiency for BIGCC plants is caused by a reason: A significant amount of fuel energy is rejected as waste heat or enthalpy in the exhaust gases at the exit of the HRSG of BIGCC resulting in the significant amount exergy expelled from the combined power cycle. Therefore, to shift towards sustainability, it is important to recover waste heat from stack gases in general and waste exergy in particular, thus reducing external emissions and thermodynamic irreversibilities [11].

Superimposition of the IGCC power plant over the organic Rankine cycle (ORC) utilizes the waste heat for additional power generation and thereby reduces the waste emissions and increases the efficiency of a combined power cycle. The ORC uses an organic working fluid to generate power. The working fluid is heated to boiling and the expanding vapour is uses to drive a turbine. The working fluid vapour is condensed back into a liquid and fed back through the system. A comprehensive discussion on thermodynamic investigation of ORC is well reported in the literature [12-13]. For these reasons, the purpose of this study is to carry out energetic and exergetic performance analyses of a biomass fuelled integrated gasification combined cycle (BIGCC) superimposed over the (ORC). A computational analysis is performed using the first and second laws of thermodynamics to investigate the

effects of some influencing parameters on the energy and exergy efficiency of combined gas-steam-ORC power cycle. For performing this analysis, first a thermo-chemical model was developed to determine the composition of syngas produced after biomass gasification. Second, a thermodynamic model was developed using the principle of conservation of mass and energy along with the second law of thermodynamics, then the defined energetic and exergetic evaluations were performed for the proposed triple power generation cycle. Solid waste and rice husk were selected as biomass materials for IGCC power cycle, and the refrigerant R-113, which is capable to recover waste heat more efficiently in the higher range of waste heat temperatures, was chosen as a working fluid for ORC.

DESCRIPTION OF THE PROPOSED CYCLE

The schematic diagram of biomass fuelled triple power cycle is shown in Figure 1. The biomass is fed to the gasifier at atmospheric conditions. The compressed air enters at (point) 2 and pressurized steam at 4 enters the gasifier. The gas produced in the gasifier after passing through a gas clean up goes to combustion chamber at 5. Gas clean up system has been shown in the schematic diagram of the proposed triple power cycle with a view that synthetic gas produced fuel gas free from particulates and alkali metals that can cause corrosion and deposition in the turbine expansion section. The synthetic gas burned in the combustion chamber in the presence of compressed air, and the combustion products at 6 goes to gas turbine where they expand and produce power. The gas turbine exhaust at 7 enters the heat recovery steam generator (HRSG) where steam is generated. The superheat steam at ‘a’, goes to steam turbine for additional power production. A part of superheat steam is extracted at an intermediate stage of turbine at ‘e’ and goes back to gasifier for biomass gasification. Saturated steam at the exit of steam turbine at ‘b’ goes to condenser where its phase changes from vapour to liquid at ‘c’. The water is then pumped to HRSG at ‘d’. The stack gases at state 8 are assumed to be 400 K [23] and routed through the evaporator where heat transfer occurs between the exhaust stream and the organic working fluids. In this study, a counter flow heat exchanger (evaporator) configuration is considered to maximize heat transfer between the stack gases at HRSG

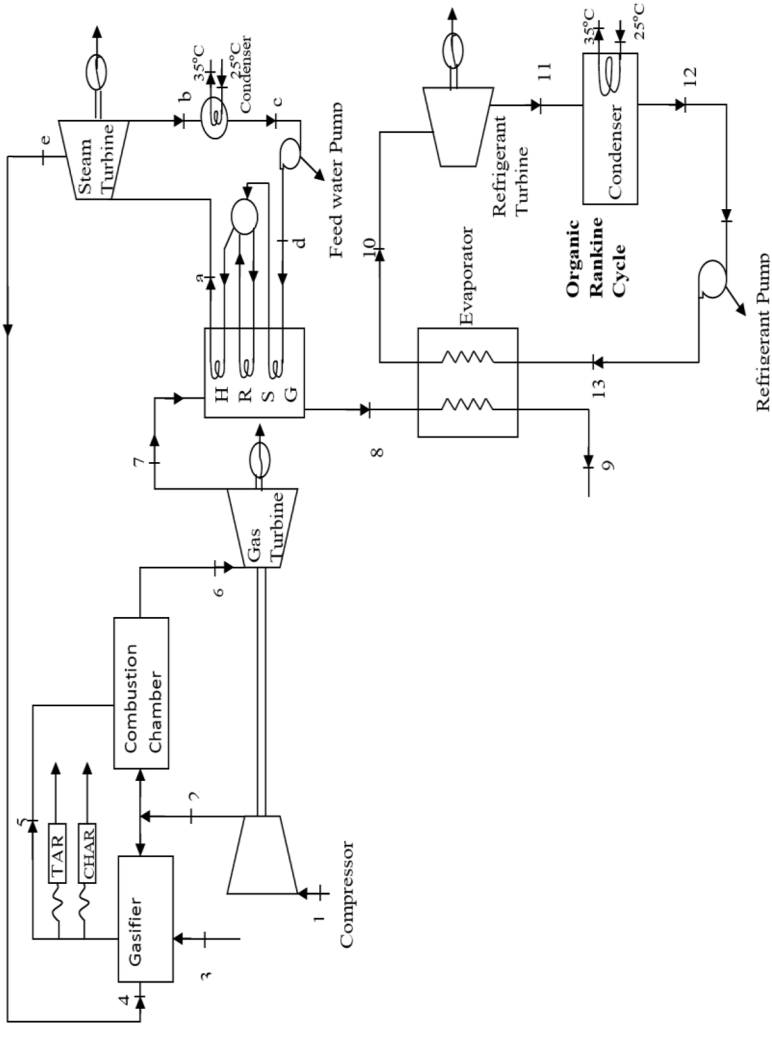

Figure 1. Schematic diagram of the proposed biomass derived syngas fuelled triple power cycle

exhaust and the organic fluid. Thermodynamically this is a preferred configuration because the temperature difference between the hot fluid and the cold fluid is minimized, thereby reducing the irreversibility. The heated organic vapour is then expanded in the turbine, heat is rejected to the ambient in the condenser, and the cooled working fluid is pumped back in to the evaporator. Stack gases at the exit of the evaporator discharge to the ambient. The mass flows of a given stream at each state are shown in Table 1.

ASSUMPTIONS

The following assumptions have been made for the analysis of the cycle [11].

Table 1. Mass of streamss at various state points

State point	Solid Waste (Mass flow in kg)	Rice husk (Mass flow in kg)
1	30.4722	28.549
2	30.4722	28.549
3	23.33	25.301
4	23.33	25.29
5	61.678	64.746
6	268.014	257.312
7	268.014	257.312
8	268.014	257.312
9	268.014	257.312
10	102.03	97.95
11	102.03	97.95
12	102.03	97.95
13	102.03	97.95
a	96.38	92.52
b	73.057	67.23
c	73.057	67.23
d	73.057	67.23
e	23.33	25.29

Table 2. Thermodynamic properties of working fluids at each state point of biomass fueled triple power cycle corresponding to the states shown in Figure 1.

Common thermodynamic properties			Solid Waste		Rice Husk	
State point	Pressure (bar)	Temperature (K)	Entropy (kJ/k)	Enthalpy (kJ/kg)	Entropy (kJ/k)	Enthalpy (kJ/kg)
1	1.013	298	205.32	302.47	205.32	302.47
2	10	624.29	212.86	666.05	212.86	666.05
3	1.013	298	89.45	1176.2	92.52	1146.42
4	10	624.29	253.1	1271.36	276.54	1271.36
5	10	1158	710.31	6321.97	757.53	6603.82
6	9.7	1238	2256.64	1890.66	2184.17	1926.81
7	1.05	885.83	2301.35	1220.69	2227.51	1245.9
8	1.013	400	2047.95	486.84	1980.25	494.21
9	1.013	246.63	468.38	444.53	468.38	444.53
10	25	350.52	172.35	429.32	172.35	429.32
11	0.44831	250.53	180.2	371.67	180.2	371.67
12	0.44831	230.53	80.06	145.66	80.06	145.66
13	25	350.52	139.99	318.18	139.99	318.18
a	40	723	851.69	3330.23	841.058	3330.23
b	0.08	314	710.936	170	640.2	170
c	0.08	314	1.814	168.77	1.814	168.77
d	100	584.04	10.577	1407.53	10.577	1407.53
e	10	624.29	253.1	1271.36	276.54	1271.36

1. Biomass fed to the gasifier at ambient conditions.
2. Air is admitted to the compressor at ambient conditions (P0 =1.013 bar, T0 =298)
3. Complete combustion takes place in combustion chamber.
4. Gasification of biomass occurs at high pressure under adiabatic condition.
5. Saturated steam extracted from the turbine enters to the gasifier at pressure equal to the compressed air pressure.
6. Steam fuel ratio (SFR) has been taken as unity.
7. Air fuel ratio (AFR) in the gasifier is assumed to be equal to 0.5.
8. Air fuel ratio in the combustion chamber is calculated for stoichiometric condition.

9. The value of gasifier temperature for selected biomass material (solid waste and rice husk) at a given gasifier pressure has been taken from the results reported by Srinivas et al. [11].
10. No pressure drops in the ORC evaporator, condenser, and pipes.
11. The unavailable stack heat transfer that takes place between the plant components and their surroundings is neglected.

ENERGETIC AND EXERGETIC ANALYSES OF TRIPLE POWER CYCLE

Performance of thermal power plants is generally evaluated through the conventional energy balance approach based on first law of thermodynamics which simply provides the overall performance in terms of power output and thermal efficiency. Energetic performance criteria, provides no information about the identification and quantification of thermodynamic losses, that occurs during the various processes in a power plant. On the other hand, exergetic performance criteria based on second law of thermodynamics determine the magnitudes, locations and causes of thermodynamic irreversibilities, occur in various components of power plants, and thereby provide insight about the potential targets for technology improvement. Exergetic analysis allows one to quantify the loss of efficiency in a process that is due to the loss in energy quality. Therefore, in the current study combined energetic and exergetic analyses have been carried out to deliver a complete depiction of power plant characteristics using the following equations of exergy and entropy:

The amount of irreversibility due to thermodynamic losses I in a steady flow device can be evaluated by considering the balance on a control volume across the device, which can be written as:

(Total exergy in) = (Total exergy out) + (Irreversibility losses) or

$$\sum m_{in} e_{in} + Q_r \left(1 - \frac{T_0}{T_r}\right) = \sum m_{out} e_{out} W + I \tag{1}$$

Where

W is the work generated by the device

Q_r is the heat transfer to the control volume
m is the amount of mass
T_0 is the reference ambient temperature
T_r is the temperature of the reservoir from which the heat transfer occur
Where, h and s represent the specific enthalpy and entropy respectively.

The second term in Equation (1) is the exergy input due to the heat transfer to the control volume. And is the exergy transfer associated with the stream of matter, and can be defined as:

$$e = (h - h_o) - T_o(s - s_o) \tag{2}$$

The irreversibility is the amount of exergy that is lost to environment and cannot be used anywhere. Assuming, that the system under consideration (fuel-air mixture) is an ideal gas, consisting of species that behave individually as ideal gases, the absolute entropy of the species 'i' at a given temperature and pressure is given by [15].

$$\bar{s}_i(T,p) = \bar{s}_i^0(P_0T_0) + \int_{T_0}^{T} \frac{\bar{C}_{pi}(T)}{T} dT - \bar{R}\ln\left(\frac{y_i p}{p_0}\right) \tag{3}$$

The absolute entropy of a mixture at a given (T, p) is given by

$$\bar{s}_{mix}(T,p) = \sum_{i=1}^{i=n} y_i \bar{s}_i(T,p) \tag{4}$$

where, $\bar{s}_i^0(P_0T_0)$ is the absolute entropy of a species 'i' in kJ/kmol-K at an ambient pressure and temperature (restricted dead state), $\bar{C}_{pi}$ is the specific heat of a species 'i' at a given temperature (T) in kJ/kmol-K, $\bar{R}$ is the universal gas constant in kJ/kmol-K, y_i is the mole fraction of species 'i' in the mixture and p is the absolute pressure of mixture and T is its temperature in K.

The specific heat of a particular species in the mixture $\bar{C}_{pi}$ (T)at a given temperature is calculated by the relation

$$\frac{C_{Pi}(T)}{R} = \alpha + \beta T + \gamma T^2 + \delta T^3 + \varepsilon T^4 \tag{5}$$

The value of constants, α, β, γ, δ and ε for a given species, are directly obtained from Eq. (5). The absolute entropy of a mixture (fluid

stream) at a given state is calculated after using Eqs. (3 and 4).The thermodynamic irreversibility in a process is characterized by entropy generation S_{gen} in the process. For continuous process performed by a system it can be written as

$$I = T_0 S_{gen} \tag{6}$$

where 'I' is the irreversibility in the process and S_{gen} is the entropy generation.

The specific heat of a mixture of gases is expressed as the sum of the specific heats of each species in the mixture and the product of their mole fractions

$$\bar{C}_{p,mix} \sum_{i=1}^{i=n} y_i \bar{C}_{pi} \tag{7}$$

DESCRIPTION OF THERMO-CHEMICAL MODEL

The general chemical formula for biomass feedstock is given by $C_{a0}H_{a1}O_{a2}N_{a3}$.

The global gasification reaction in the biomass gasifier can be written as

$$C_{a0}H_{a1}O_{a2}N_{a3} + wH_2O + a_4\,(O_2 + 3.76N_2) + a_5H_2O \rightarrow$$
$$b_1CH_4 + b_2CO + b_3CO_2 + b_4H_2 + b_5H_2O + b_6N_2 \tag{8}$$

where C, H, O and N are the fuel mass fractions from the ultimate analysis on dry basis. For single-carbon-atom fuel (a_0=1), the coefficients a_1, a_2 and a_3 are determined from H/C, O/C and N/C mole ratios respectively.

The reactions are solved at thermodynamic equilibrium. The gasification products contained CH_4, CO, CO_2, H_2, H_2O, and N_2.

$$a_1 \quad \frac{(H/M_H)}{(C/M_C)} \tag{9}$$

$$a_2 \quad \frac{(O/M_O)}{(C/M_C)} \tag{10}$$

$$a_3 \quad \frac{(N/M_N)}{(C/M_C)} \tag{11}$$

Molecular weight of dry fuel

$$M_{dry\ fuel} = A_1 M_{CH} + a_2 M_O + a_3 M_N \tag{12}$$

then

$$W = \frac{M_{dry\ fuel} m_C}{M_{H_2O}\,(100 - m_C)} \tag{13}$$

Molecular weight of wet fuel

$$M_{wet\ fuel} = M_{dry\ fuel} + wM_{H_2O} \tag{14}$$

Stoichiometric air fuel ratio

$$SAFR = \frac{(a_1 + 0.25a_2 - 0.5a_S)M_A}{M_{wet\ fuel}} \tag{15}$$

where
$M_A = M_{O_2} + 3.76M_{N_2}$

$$a_4 = \frac{SFR \times M_{wet\ fuel}}{M_A} \tag{16}$$

$$a_5 = \frac{SFR \times M_{wet\ fuel}}{M_{H_2O}(1–0.01 \times A)} \tag{17}$$

In Eqs. (19, 20) a_4 and a_5 are obtained. A numerical method is applied to solve the syngas coefficient in steam gasification by using Taylor's series method [11]. After completion of numerical iteration at AFR = 0.5, SFR = 1 and gasifier pressure = 10 bars, the syngas composition is shown in Table 3.

The complete combustion equation for the syngas in the GTCC with the compressed air is

Table 3. Thermo-chemical properties of biomass materials [11]

Property	Units	Solid Waste	Rice Husk
C	Wt% daf	51.03	36.42
H	Wt% daf	6.77	4.91
O	Wt% daf	39.17	35.88
N	Wt% daf	2.64	0.59
Lower Heating Value	kJ/kg,daf	25021.51	22982.32
Moisture Content	Wt%	15.00	15.00
Ash	Wt%	5.00	22.20

$$b_1CH_4 + b_2CO + b_3CH_2 + b_4H_2 + b_5H_2O + b_6N_2 + a_7(O_2 + 3.76N_2) \rightarrow b_7CO_2 + b_7CO_2 + b_8H_2O + b_9N_2 + O_2 \quad (18)$$

In Eq. (21) 'a_7' is the amount of air to be supplied in kg-mol (stoichiometric air for combustion) into the GTCC.

The amount of air required for combustion to obtain the required temperature (T) is determined from the energy balance of reactants and products. Following are the products required in the GTCC at the above mentioned condition which may be computed after species balance on R.H.S. and L.H.S. in Tables 4 and 5.

The calorific value of synthetic gas (Q_{cv} or LHV) at a given combustion outlet temperature may be obtained after making energy balance over the combustion chamber, and the desired equation may be given as

$$\Sigma_R\left(\bar{h}_f^0 + \Delta\bar{h}\right) + \bar{Q}_{cv} = \Sigma_P\left(\bar{h}_f^0 + \Delta\bar{h}\right) \quad (19)$$

The equations for computing the irreversibility in each component of the proposed triple cycle generation system, other than gasifier and combustion chamber, can be developed, after using the Eqs. (1-4), and may appear in the following form:

$$I_C = W_C + m_a e_1 - m_a e_2 \quad (20)$$

$$I_{GT} = m_{mix}\,(e_6 - e_7) - W_{GT} \quad (21)$$

$$I_{\text{HRSG}} = m_{mix}\,(e_7 - e_8) + m_{H2)}(e_d - e_a) \quad (22)$$

Table 4. Properties and operating variables for the analysis of the proposed cycle—ORC configuration [3, 14]

Properties of Ambient Air	
Pressure (bar)	1.013
Temperature (K)	298
Composition (by volume)	
Nitrogen	79%
Oxygen	21%
Equipment Performance	
Isentropic efficiency of compressor ($\eta_{c,isen}$)	85%
Isentropic efficiency of gas turbine ($\eta_{gt,isen}$)	85%
Isentropic efficiency of steam turbine ($\eta_{st,isen}$)	85%
Pressure drop across the gasifier (ΔP_G)	5%
Pressure drop across the combustion chamber (ΔP_{CC})	3%
Pressure drop across the HRSG (ΔP_{HRSG})	2%
Operating Parameters	
Compressor pressure ratio (r_p)	6–14 (range)
Turbine inlet temperature TIT (^{0}C)	970–1050 (range)
Condenser outlet pressure (bar)	0.06
Feed water pump pressure (bar)	0.06
Stack temperature after HRSG (K) (assumed)	400
Working fluid of ORC	R-113
ORC turbine inlet pressure (MPa)	1.5–3.5 (range)
ORC turbine outlet pressure (MPa)	0.044831
ORC turbine isentropic efficiency	80%
ORC pump isentropic efficiency	85%
Pinch point temperature	20-30 K (range)
Approach temperature	15ºC
Steam to fuel ratio = unity (assumed)	SFR=1
Relative air fuel ratio = $\frac{\left(\frac{A}{F}\right)act}{\left(\frac{A}{F}\right)stoich} = (RAFR = 0.1)$ (assumed)	RAFR=0.1

$$I_{ST} = m_a e_a - m_e e_e - m_b e_b - W_{ST} \tag{23}$$

$$I_{SC} = m_b\,(e_b - e_c) \tag{24}$$

$$I_{FP} = m_c\,(e_{12} - e_{13}) + W_{Fp} \tag{25}$$

$$I_{pump} = T_0 m_f (s_{13} - s_{12}) \tag{26}$$

Table 5. Composition of synthetic gas produced after gasification and exhaust gas after composition for one kmol of biomass at pressure ratio (r_p=10)

Constituent	Solid Waste Concentration (kmol)	Rice Husk Concentration (kmol)
Synthetic Gas		
CH_4	b1=0.16	b1=0.06
CO	b2=0.52	b2=0.62
CO_2	b3=0.32	b3=0.31
H_2	b4=0.84	b4=0.99
H_2O	b5=0.94	b5=1.12
N_2	b6=0.44	b6=0.39
Exhaust Gas (Combustion Product)		
CO_2	b7=1	b7=1
H_2O	b8=2.1	b8=2.23
N_2	b9=6.08	b9=5.65
O_2	0.5	0.47
a_7	1.5	1.4

$$I_e = T_0 m_{vapour}\left[(s_{10} - s_{13}) - \frac{(h_{10} - h_{15})}{T_H}\right] \quad (27)$$

$$I_{T,ORC} = T_0 m_{vapour}(s_{11} - s_{10}) \quad (28)$$

$$I_{IC} = T_0[m_{vapour}(s_{12} - s_{11}) + m_{coolant}(s_{hot\ water,\ out} - s_{cold\ water,in})] \quad (29)$$

PERFORMANCE PARAMETERS

First-law (energy) efficiency (η_I)

The thermal efficiency is defined as the ratio between the net power output of the cycle to the heat input, which may be expressed as:

$$\eta_I = \frac{W_{GT} + W_{ST} + W_{T1ORC} - W_{AC} - W_P - W_{P1ORC}}{m_f LHV} \quad (30)$$

Where m_f is the mass of fuel consumed.

Exergy efficiency (η_{II})

The amount of exergy supplied in the product to the amount of exergy associated with the fuel is a more accurate measure of this

thermodynamic parameter of a system. By definition, the second law efficiency is then given by the following expression:

$$\eta_{II} = \frac{W_{GT} + W_{ST} + W_{T1ORC} - W_{AC} - W_P - W_{P1ORC}}{E_{fuel,in}} \quad (31)$$

where $E_{fuel,in}$ is the exergy of fuel.

RESULTS AND DISCUSSION

A biomass derived syngas fuelled triple cycle power generation system is proposed, and both energetic and exergetic analyses, are performed in the current study. The analysis involves the determination of first and second law efficiencies of the triple cycle and computation of irreversibility in the individual component of the cycle using the thermodynamic model which was developed with the Engineering Equation Solver (EES) Software [16]. The range of pressure ratio across the compressor and gas turbine inlet pressure were assumed (6-14) and (970°C-1050°C), respectively.

The effect of change in the gas turbine inlet temperature on first law efficiency of combined power cycle is shown in Figure 2(a) which shows that first law efficiency increases with the increase in gas turbine inlet temperature due to obvious reasons. Increase in combustor outlet temperature results in the increase of mean temperature of heat addition which leads to the reduction in amount of syngas required for power generation and hence results in the increase of first law efficiency. It also shown that first law efficiency of solid waste fuelled is significantly higher than the first law efficiency of combined power cycle of rice husk fuelled combined power cycle. This is because the energy content (LCV) of solid waste is considerably higher than the energy content of rice husk.

Figure 2 (b) shows the effect of change in turbine inlet temperature on first law efficiency of triple power cycle. It is observed that first law efficiency increases with the increase in turbine inlet temperature and it is slightly greater than its combined cycle counter part due to the recovery of waste heat at exit of HRSG which produced additional power through the turbine of ORC. Solid waste fuelled triple power

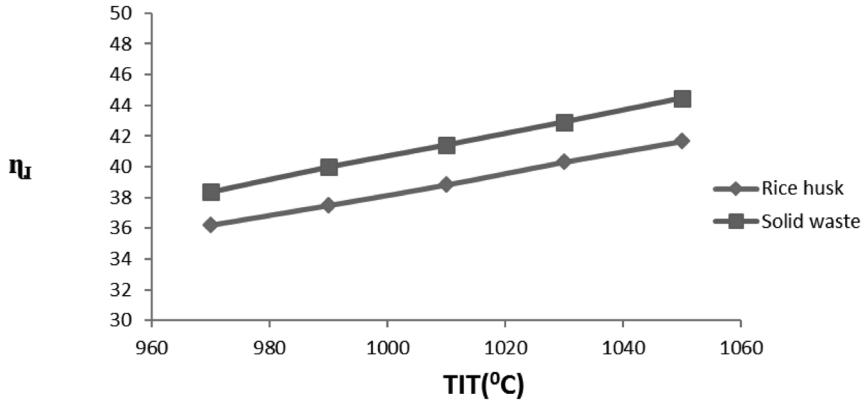

Figure 2 (a). Variation of first law efficiency of combined power cycle with the turbine inlet temperature at (r=10)

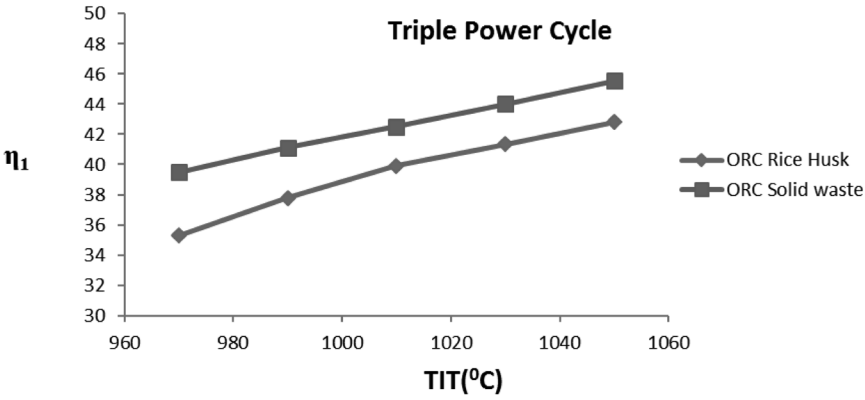

Figure 2 (b). Variation of first law efficiency of triple power cycle with the turbine inlet temperature at (r=10)

cycle provides better first law efficiency than the rice husk fuelled triple cycle.

Application of principle of increase of entropy over the various components of biomass fuelled combined power cycle results in the evaluation of irreversibilies, which in turn, determine the second law efficiency of the cycle that provides a more meaningful assessment. The effect of gas turbine inlet temperature on second law efficiency of the cycle is shown in Figure 3(a) and it is observed that second law

efficiency increases with the increase in gas turbine inlet temperature for both the fuels due to the reason that, higher combustor outlet temperature (gas turbine inlet temperature) results in lesser entropy generation during combustion which is a major source of irreversibility in the cycle and hence it leads to an increase in second law efficiency with the increase in gas turbine inlet temperature. It is further shown that second law efficiency of solid waste fuel combined cycle is higher than the second law efficiency of the rice husk fuel combined cycle at same gas turbine inlet temperature. This is because the exergy content of solid waste biomass is considerably lower than the exergy content of rice husk biomass.

The effect of gas turbine inlet temperature on second law efficiency of triple power cycle is depicted in Figure 3(b) which shows that recovery of the exergy of waste heat at the exit of HRSG of BIGCC using the ORC increases its second law efficiency by a smaller amount. Since the exergy content of waste heat at exit of HRSG is less than its energy content, therefore, the second law efficiency of triple power cycle is less than its first law efficiency. The same can be visualized after comparing of Figs 3(a) and 3(b).

Figure 4 (a) shows the variation of first law efficiency of biomass fuelled combined power cycle for a fixed gas turbine inlet temperature (TIT=1010°C). It is observed that as pressure ratio across the compressor (gasifier pressure) increases, the first law efficiency increases.

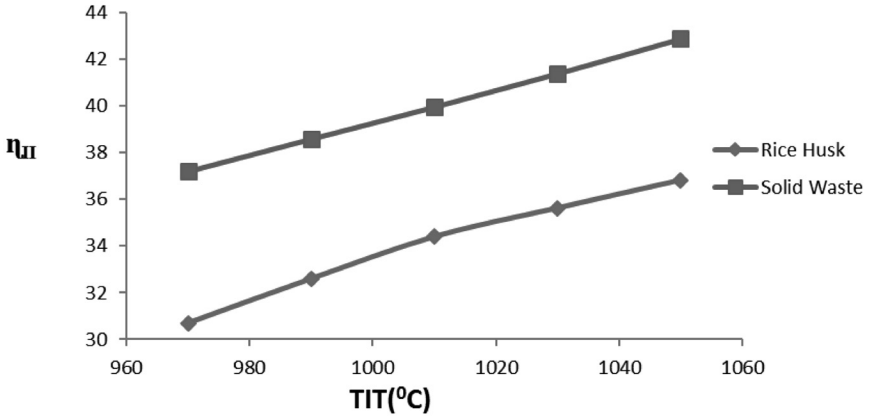

Figure 3 (a). Variation of second law efficiency of combined power cycle with the turbine inlet temperature at (r=10)

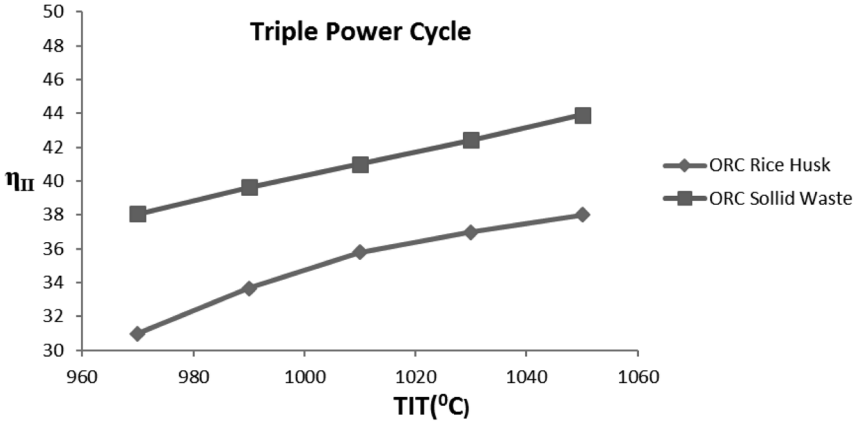

Figure 3 (b). Variation of second law efficiency of triple power cycle with the turbine inlet temperature at (r=10)

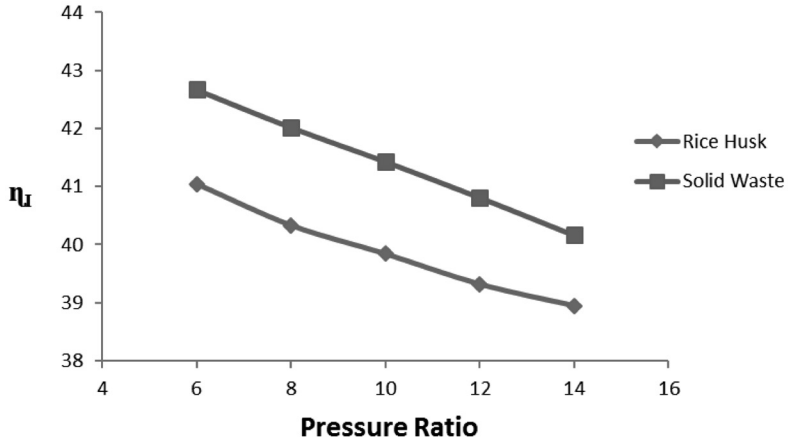

Figure 4 (a). Variation of first law efficiency of combined power cycle with the pressure ratio at (TIT=1010°C)

This is due to the fact that increase in pressure ratio increases the amount of work delivered by the gas turbine at a fixed inlet temperature which simultaneously lowers the enthalpy of steam generated in the HRSG, and hence, reduces the work delivered by the steam turbine which decreases the overall work output of the cycle at a given heat input (LHV) of biomass that enters the gasifier at ambient condition. The first law efficiency values with the pressure ratio shows a trend similar to the one reported by [4] for coal as a primary fuel. Due to the higher

energy content of solid waste biomass its first law efficiency is higher than the first law efficiency of rice husk biomass of the combined power cycle and similar trend is observed for the first law efficiency with the increase in the pressure ratio for both biomass materials.

The effect of change in pressure ratio across the compressor on first law efficiency of triple power cycle is shown in Figure 4(b). It is found that first law efficiency of triple power cycle is showing the trend similar to the combined power cycle with respect to pressure ratio. Utilization of waste heat at the exit of the HRSG results in the enhanced performance of the combined power cycle. It is further shown that the first law efficiency of solid waste fuel triple power cycle is higher than the first law efficiency of rice husk biomass fuel cycle due to the larger energy content of solid waste biomass.

The effect of pressure ratio across the compressor on second law efficiency of combined power cycle is shown in Figure 5(a). It is observed that the second law efficiency of both biomass fuels (solid waste, rice husk) combined cycle decreases with the increase in pressure ratio. This is due to the following:

First increase in gasifier pressure results in the higher gasifier temperature which increases the irreversibility due to the heat transfer at the finite temperature difference that results in the larger irreversibility in the gasifier. Second the exergy content of synthetic gas increases with the increase in gasifier pressure. Due to these two combined effects a

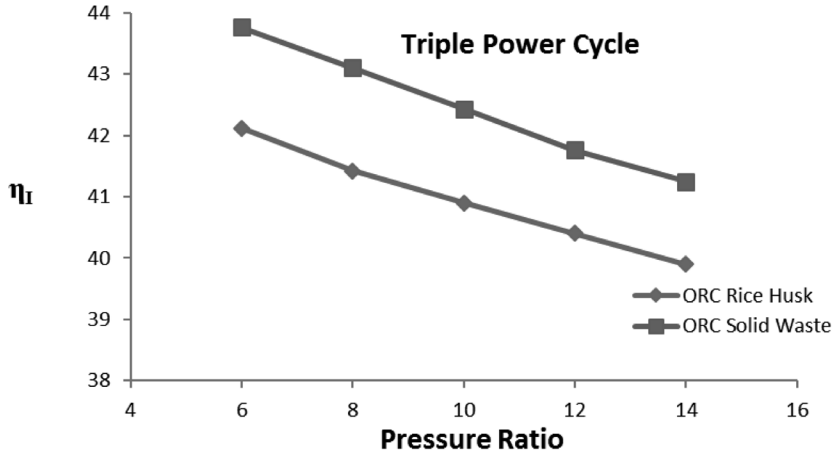

Figure 4 (b). Variation of first law efficiency of triple power cycle with the pressure ratio at (TIT=1010°C)

reduced second law efficiency of combined power cycle is observed at higher pressure ratio. The second law efficiency of solid waste fuel combined cycle is found to be considerably greater than the second law efficiency of rice husk fuel cycle due to the lower exergy content of solid waste fuel than rice husk.

Figure 5(b) shows the same trend of decreasing second law efficiency with the increase in pressure ratio for triple power cycle. This is because increase in pressure ratio consequently increases the irre-

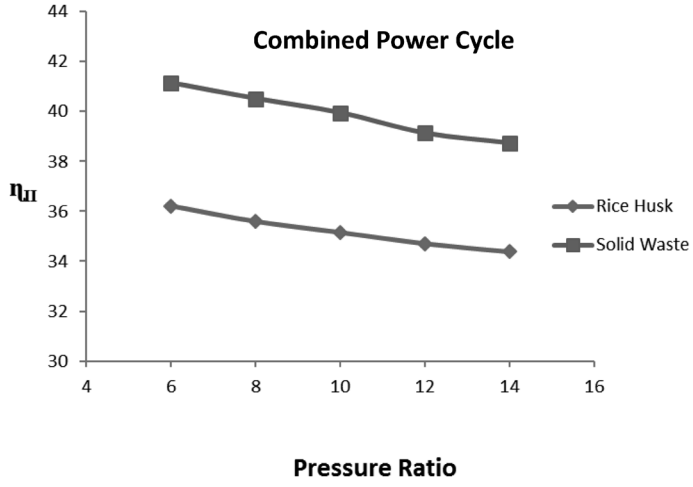

Figure 5 (a). Variation of second law efficiency with pressure ratio of combined power cycle (TIT=1010°C)

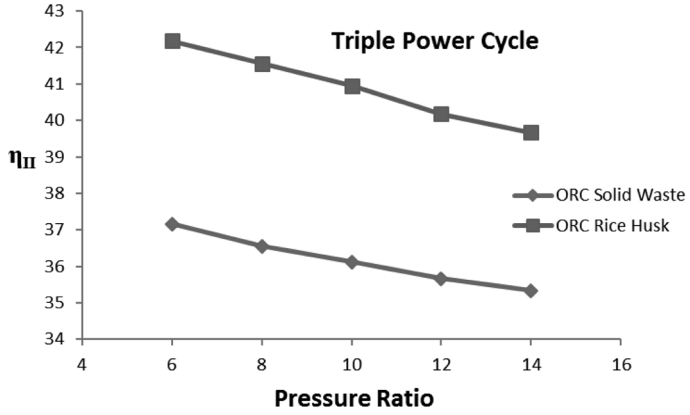

Figure 5 (b). Variation of second law efficiency of triple power cycle with the pressure ratio (TIT=1010°C)

versibility in the evaporator and condenser in the ORC along with the increase in irreversibility in gasifier and combustor in combined power cycle. Simultaneous increase in irreversibility of the key components of the triple power cycle results in the reduced second law efficiency of triple power cycle.

Keeping in view the potential benefits of exergetic analysis over the energetic analysis described above a thermodynamic model has been applied to identify and quantify the sources of irreversibilities in various components of the proposed cycle that dictates which component needs much more attention to improve the performance of the cycle. Figure 6(a) show the exergy destruction in solid waste fuelled triple power cycle. The exergetic analysis of the solid waste driven triple power cycle clearly indicates that maximum irreversibility occurs in the combustion chamber which is around 25% of the fuel exergy input. This is due to the fact combustion is a highly irreversible phenomena where entropy is generated via heat conduction, chemical reaction, viscous dissipation and mass diffusion.

The second largest irreversibility occurs in HRSG which is around 19% of the fuel input exergy, due to significant entropy generation via heat transfer at a finite temperature difference between the two fluid streams of very high and very low temperature. The next larger irreversibility occurs in gasifier which is around 7.6% due to partial combustion process in the gasifier via the occurrence of simultaneous oxidation and reduction reactions. Partial combustion contributes towards larger irreversibility due to significant entropy generation into the gasifier. The irreversibility in gas turbine and steam turbine found to

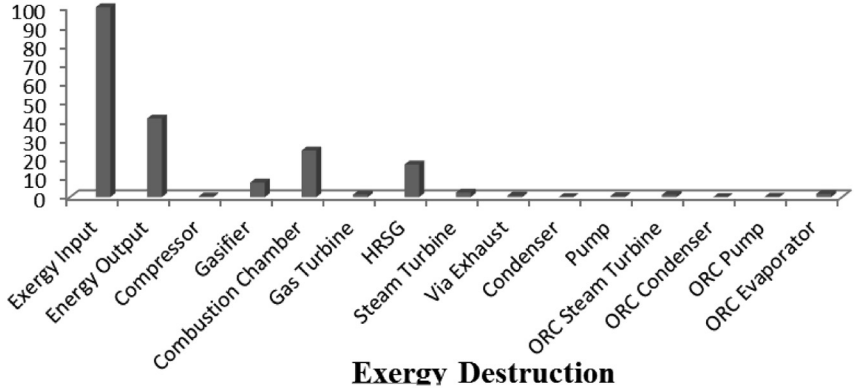

Figure 6(a). Exergy destruction in solid waste fuelled triple power cycle

be into the range (2%-3%) due to less irreversible expansion process in the two turbines. The irreversibility in other component of triple power cycle is shown to be negligible. Figure 6(b) presents the exergy destruction in rice husk fuelled triple power cycle. Almost similar trends for irreversibility in various components of rice husk driven triple power cycle are observed. The amount of exergy of fuel available as work output is slightly higher in solid waste fuelled triple power cycle than its rice husk counter part due to the greater exergy content of solid waste than rice husk.

CONCLUSIONS

A biomass derived syngas fuelled triple cycle power generation system has been developed and analysed through the cascade utilization of energetic and exergetic approaches. Based on the analysis, the following findings are obtained:

- A considerable variation in both first and second law efficiencies of the triple power cycle was observed with the change in pressure ratio and gas turbine inlet temperature.
- For mean operating conditions, the first and second law efficiencies of solid waste fuelled triple power cycle were found to be 42.51% and 40.99%, respectively, whereas for rice husk fuelled

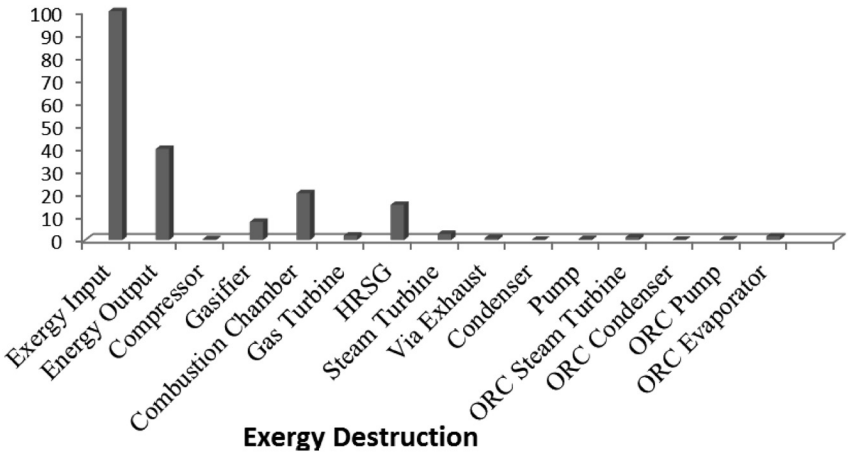

Figure 6(b). Exergy destruction in rice husk fuelled triple power cycle

triple power cycle these efficiencies were of the values of 40.92% and 36.12%, respectively.

- Exergetic analysis of the proposed triple power cycle reveals the magnitude of irreversibility in the combustor, HRSG, and gasifier as; 25%, 19% and, 7.6%, respectively.

Employment of ORC as a bottoming cycle to BIGCC shows a moderate improvement in its thermal performance.

- Overall, the obtained results show that the variations in system operating parameters directly influence the irreversibility in the components and first and second law efficiencies of the cycle. Proposed triple power cycle shows the bright prospects of improved system integration for sustainable power generation using biomass as a primary energy source.

Nomenclature

AFR	Air fuel ratio
C	Compressor
CC	Combustion Chamber
ED	Exergy destruction (kJ/kg-K)
FP	Feed pump
G	Gibbs function (kJ/kg-mol)
GT	Gas turbine
HRSG	Heat recovery steam generator
I	Irreversibility
LHV	Lower heating value (kJ/kg)
M	Molecular weight
m	Mass (kg)
m_{vapour}	Mass of refrigerant (R-113) vapour in ORC
N	Nitrogen
O	Oxygen
ORC	Organic Rankine cycle
P	Product, pump
p	Pressure (bar)
Q	Heat transfer interaction (J)

Q_{cv}	Calorific value (kJ/kg)
R	Reactant
$\overline{R}$	Universal gas constant (kJ/kg-mol)
$r_{p,C}$	Pressure ratio across the compressor
$r_{p,\,GT}$	Pressure ratio across the gas turbine
SAFR	Stoichiometric air fuel ratio
SFR	Steam fuel ratio
ST	Steam turbine
s	Specific entropy (kJ/kg-K)
S_{gen}	Entropy generation
T	Absolute temperature (K)
T_0	Atmospheric temperature (K)
T_p	Saturated temperature at pressure of process steam (K)
W	Work (kJ/kg)
w	No. of moles of moisture in the biomass

Suffixes

a-e	State points of the steam cycle
bmf	Biomass fuel
ch	Chemical
d.a.f.	Dry ash free
e	Specific exergy (kJ/kg)
f	Formation
$\overline{g}$	Gibb's free energy (kJ/kg mol)
h	Specific enthalpy (kJ/kg)
h_c	Enthalpy of condensate return (kJ/kg)
h_f	Enthalpy of saturated water at process steam pressure (kJ/kg)
h_g	Enthalpy of saturated vapour at process steam pressure (kJ/kg)
ph	Physical
$\Delta\overline{h}$	Change in enthalpy (kJ/kg mol)
$\overline{\beta}$	Pressure drop factor
$\alpha, \beta, \gamma, \delta, \varepsilon$	Constants

0	Reference point
1-13	State points of the gas-steam cycle
(-)	Per mol
η_I	First law efficiency
η_{II}	Second law efficiency

References

[1] Filho P.A. and Badr O., 2004. Biomass resources for energy in northeastern Brazil. *Applied Energy* 77, 51-67.

[2] Ahmadi P., Dincer I., Rosen M.A., 2014. Thermoeconomic multi-objective optimization of a novel biomass-based integrated energy system. *Energy* 68, 958-970.

[3] Franco A and Giannini N., 2005. Perspectives for the use of biomass as fuel in combined cycle power plants. *Int. J. Thermal Sci* 44,163-177.

[4] Hasegawa T and Tamaru T., 2007. Gas turbine combustion technology reducing both fuel NO_x and thermal-NO_x emissions for oxygen blown IGCC with hot/dry synthetic gas clean up. *Journal of Engineering for Gas Turbines and Power* 129, 358-369.

[5] Mark A and Mike J.W., 2003. Biomass gasification combined cycle opportunities using the future energy Silvas gasifier coupled to Alstom's industrial Gas Turbines. ASME papers no GT 2003-38294.

[6] Prins M.J., Ptasinski K.J., Janssen F.J.J.G., 2007. From coal to biomass gasification. Comparison of thermodynamic efficiency. *Energy*, 32, 1,248-1,259.

[7] Ptasinski K.J., Prins M.J. and Pierik A., 2007. Exergetic evaluation of biomass gasification. *Energy*, 32(4), PP.568-574.

[8] Rutherford J., 2006. Heat and power applications of advanced biomass gasifiers in New Zealand's wood industry. M.E. thesis in chemical and process engineering, University of Canterbury, Christchurch, New Zealand.

[9] Bhattacharya Abhishek., Manna Dulal., Paul, Bireswar., Data Amitava., 2011. Biomass integrated gasification combined cycle power generation with supplementary biomass firing: Energy and exergy based performance analysis. Energy 36, 2,599-2,610.

[10] Fagbenle R., Layi, Oguaka A.B.C., Olakoyejo O.T., 2007. A thermodynamic analysis of a biogas-fired integrated gasification steam injected gas turbine (BIG/STIG) plant. *Applied Thermal Engineering* 27 pp. 2,220-2,225.

[11] Srinivas T., Gupta A.V.S.S.K.S., Reddy B.V., 2009. Thermodynamic equilibrium model and exergy analysis of a biomass gasifier. *Journal of energy resources technology*.Vol.131/031801-7.

[12] Somayaji C., Mago, P.J. and Chamra., L.M., 2006. Second law analysis and optimization of organic Rankine cycle. ASME power conference, Atlanta, GA, paper no PWR 2006-88061.

[13] Ahmadi P., Dincer I., Rosen M.A., 2012. Exergo-environmental analysis of an integrated organic Rankine cycle for trigeneration. *Energy Conversion and Management* 28 pp.998-1007.

[14] Mago P.J, Srinivasan K.K., Chamra L.M., and Somayaji., 2008. An examination of exergy destruction in organic Rankine cycle. Int. J. Energy Res., 32pp 926-938.

[15] Khaliq A., 2015. Energetic and exergetic performance evaluation of a gas turbine power cogeneration system using reverse Brayton refrigeration cycle for inlet air cooling. Transactions of the American Society of Civil Engineers—Journal of Energy Engineering DOI: 10.1061/(ASCE) EY.1943-7897.0000290, USA

[16] Klein SA, Alvarado F. Engineering equation solver. Version 7.441, F-Chart Software 2005; Middleton.

ABOUT THE AUTHORS

Faizan Ahmad has done his M.Tech in Chemical Engineering (Process Modeling and Simulation) from Aligarh Muslim University, Aligarh. He has three years of teaching experience in the department of Chemical Engineering, Aligarh Muslim University, Aligarh. He is working as assistant professor in the department of Post Harvest Engineering and Technology, Faculty of Agricultural Sciences, Aligarh Muslim University, Aligarh. He has published technical articles in various journals of international repute. His area of interest is heat transfer, fluid mechanics, computational fluid dynamics and food processing. Email: f4faizahmad1989@gmail.com.

Abdul Khaliq, corresponding author, has a Ph.D. in thermal engineering from IIT Delhi and post doctoral research in energy engineering from UOIT Canada. He is working as a professor of mechanical engineering at King Fahd University of Petroleum and Minerals, Dhahran, Saudi Arabia. He has guided 7 Ph.D. theses as a sole supervisor and published a large number of research papers in various peer reviewed journals of international repute. His research referenced internationally with an H-index of 15. He has won many awards from the government of India for his excellent teaching and research record. Emails: akhaliq@kfupm.edu.sa, khaliqsb@gmail.com Tel.: +966 561303088.

Mohammad Idrees received his Ph.D. in chemical engineering from IIT Kanpur. He is a professor of chemical engineering and chairperson of the Department at Aligarh Muslim University, India. His teaching experience spans more than three decades including those at IIT Kanpur (as SRA and TA) and five years at University Technology Malaysia, Kuala Lumpur, and Johor Bahru. Current activities of his research group focus on hazardous waste management, nanocomposite synthesis, mathematical modeling and simulation, reaction engineering, energy studies and process integration. He has been principal investigator of many major research projects, has supervised 5 PhDs and published numerous research papers in journals of international repute. Email: idreesingenieur@gmail.com.